Local Dynamics in Trained Recurrent Neural Networks

Alexander Rivkind[1,2,*] and Omri Barak[1,2,†]
[1]Faculty of Medicine, Technion–Israel Institute of Technology, Haifa 32000, Israel
[2]Network Biology Research Laboratories, Technion–Israel Institute of Technology, Haifa 32000, Israel
(Received 18 December 2015; revised manuscript received 5 March 2017; published 23 June 2017)

Learning a task induces connectivity changes in neural circuits, thereby changing their dynamics. To elucidate task-related neural dynamics, we study trained recurrent neural networks. We develop a mean field theory for reservoir computing networks trained to have multiple fixed point attractors. Our main result is that the dynamics of the network's output in the vicinity of attractors is governed by a low-order linear ordinary differential equation. The stability of the resulting equation can be assessed, predicting training success or failure. As a consequence, networks of rectified linear units and of sigmoidal nonlinearities are shown to have diametrically different properties when it comes to learning attractors. Furthermore, a characteristic time constant, which remains finite at the edge of chaos, offers an explanation of the network's output robustness in the presence of variability of the internal neural dynamics. Finally, the proposed theory predicts state-dependent frequency selectivity in the network response.

DOI: 10.1103/PhysRevLett.118.258101

Task learning is considered the *raison d'etre* of recurrent neural networks (RNNs), studied in the context of neuroscience and machine learning [1,2]. Yet, a theoretical understanding of trained RNN dynamics is lacking, with most of the existing physics literature addressing either random networks [3–7], designed networks [8–10], or a designed control setting [11–13].

In this Letter, we advance a theory of trained RNN dynamics. We consider an initially random, chaotic network whose output is trained to produce several target values and then fed back to the network, yielding multiple fixed point attractors. This setting underlies complex tasks that were analyzed phenomenologically using rate models [1,14,15] and are the subjects of attempts [16] to extend to more realistic task performing networks [17]. Using a mean field analysis, we derive the effect of training on the output dynamics in the vicinity of the training targets. The resulting dynamics are qualitatively different from those induced by a random modification of the same form and magnitude as induced by training [18]. The stability, which is a critical property for such training [19], is then assessed, showing that training success depends on the network's nonlinearity. Next, we show that multiple training targets can lead to state-specific frequency selectivity, as observed in task-adapted biological neuronal circuits [20,21]. Finally, the settling time of an output of a perturbed RNN is shown to remain *finite* at the edge of the chaos, contrary to the varying internal state dynamics [22,23], for which the settling time is known to diverge [3].

Model and training protocol.—Reservoir computing [24,25] is a popular and simple paradigm for training RNNs. A network of neurons with random recurrent connectivity (referred to as the reservoir) is equipped with readout weights trained to produce a desired output while keeping the rest of the connectivity fixed. The dynamics [3–5,26] are given by

$$\dot{x} = -x + Wr + w_{\mathrm{FB}} z + w_{\mathrm{in}} u \tag{1}$$

with state $x \in \mathbb{R}^N$ representing the synaptic input and the firing rate given by $r(t) = \phi(x(t))$, where $\phi(x)$ is an elementwise nonlinear function of x, commonly set to $\phi(x) = \tanh(x)$. Output $z = w_{\mathrm{out}}^T r(t)$ and input $u(t)$ are fed into the network via weight vectors w_{FB}(respectively, w_{in}) $\in \mathbb{R}^N$ with elements independent identically distributed. Elements of the connectivity matrix $W \in \mathbb{R}^{N\times N}$ are independent identically distributed as $W_{ij} \sim \mathcal{N}(0, g^2 N^{-1})$ with g being a gain parameter.

The goal of the training process is to have the output $z(t)$ approximate some predefined target function $f(t)$. In the echo state training method [25], one breaks the readout-feedback loop, creating an auxiliary open loop system defined as

$$\dot{x} = -x + Wr + w_{\mathrm{FB}} f + w_{\mathrm{in}} u, \tag{2}$$

in which the target function $f(t)$, rather than the readout $z(t) = w_{\mathrm{out}}^T r(t)$, is injected via the feedback weights w_{FB}. If this open loop system is globally stable, linear regression can be used to find w_{out} so that $z_{\mathrm{OL}} = w_{\mathrm{out}}^T r \approx f$, which becomes exact for large networks. While open loop stability, known as the fading memory property, is assumed in both echo state and first-order reduced and controlled error training [25–27], the Achilles heel of the training procedure is the subsequent transition back to the closed loop dynamics (1). Here instability can arise and a variety of other phenomena may emerge. Fortunately, the randomness of the internal connections and their intactness during the training enable a detailed analysis of the trained network as reported in what follows.

Dynamics of a trained network.—Here, we assume zero input ($u \equiv 0$) and train the network to have $M \ll N$ fixed points of (1), corresponding to constant output levels $z \in \{A_1, \ldots, A_M\}$ with respective solutions $\bar{x}_1, \ldots, \bar{x}_M$ and rates $\bar{r}_1, \ldots, \bar{r}_M$.

For a given target $f(t) \equiv A$, fading memory implies that the open loop system (2) converges to a unique stable state $\bar{x}$, given by

$$\bar{x} = W\phi(\bar{x}) + w_{\mathrm{FB}}A, \tag{3}$$

and that the spectral radius ρ of the linearized open loop dynamics WR', given by $\rho^2 = g^2\langle r'^2\rangle$ [7,18], is smaller than *one*. Here $R'_{ij} = \delta_{ij}r'_i$ with $r' = \phi'(\bar{x}) = (d\phi/dx)|_{x=\bar{x}}$ is a diagonal matrix of linearized rate functions. The average $\langle . \rangle$ is taken over neurons and by the mean field theory (MFT) assumption equals the ensemble average over realizations of W.

Importantly, asymptotic stability of the open loop system (2) does not guarantee stability of the *closed loop* system (1). This can be understood by considering the linearization of the latter:

$$\delta\dot{x} = [-I + (W + w_{\mathrm{FB}}w_{\mathrm{out}}^T)R']\delta x. \tag{4}$$

For large N, the resulting spectrum consists of a disklike spectral density region of radius ρ associated with WR' as in the open loop system and other eigenvalues related to the feedback loop term $w_{\mathrm{FB}}w_{\mathrm{out}}^T$. We will show that exactly M eigenvalues correspond to the latter and that their loci can fall either inside or outside the spectral density disk. Figure 1 shows how these loci determine the stability, convergence times, and oscillations for networks that comply with fading memory.

We will derive these eigenvalues of the closed loop system by analyzing the open loop gain—the response of the open loop output to a small perturbation in the drive $f = A + \delta f(t)$. In the Fourier domain, the state perturbation $X(\omega)$ is given by

$$i\omega X(\omega) = -X(\omega) + WR'X(\omega) + w_{\mathrm{FB}}F(\omega), \tag{5}$$

leading to the open loop gain:

$$G^{\mathrm{OL}}(\omega) = Z[\omega|F(\omega) \equiv 1] = w_{\mathrm{out}}^T R' X[\omega|F(\omega) \equiv 1]. \tag{6}$$

Poles of (6) correspond to the spectrum of the linearized open loop system, and we thus expect N poles. We will show, however, that the mean field estimate for (6) is of the order $M \ll N$. This fact should be interpreted as a lack of *observability* [32] of all except M linear modes of the network. Algebraically, it means that $N - M$ out of the N poles of $G^{\mathrm{OL}}(\omega)$ are canceled by zeros. Consequently, since the closed loop gain is given by

$$G^{\mathrm{CL}}(\omega) = G^{\mathrm{OL}}(\omega)[1 - G^{\mathrm{OL}}(\omega)]^{-1}, \tag{7}$$

only loci of M eigenvalues are updated when closing the loop, while the rest of the spectrum remains unchanged.

This finding is far from being obvious *a priori*: Closing the loop is equivalent to a rank one perturbation $w_{\mathrm{FB}}w_{\mathrm{out}}^T$ in (4). On the one hand, such a perturbation with an appropriately chosen w_{out} could, in principle, arbitrarily modify all the eigenvalues of the spectrum [27]. On the other hand, for a case of w_{out} independent of the initial connectivity matrix W, only one eigenvalue will change, as follows from a formula for spectral density devised in Ref. [18].

Single training target.—We estimate $G^{\mathrm{OL}}(\omega)$ for $N \to \infty$ and $M = 1$ using second-order statistics of $\bar{x}$ and X. Following the notation in Ref. [4], we denote the deterministic (independent of W) part of the solution $\bar{x}$ of (3) by $\bar{x}^0$ and the stochastic one by $\bar{x}^1$. Namely, we have $\bar{x}^0 = w_{\mathrm{FB}}A$ and $\bar{x}^1 = W\phi(\bar{x})$ with elements $\bar{x}_i^1$ distributed as $\bar{x}_i^1 \sim \mathcal{N}(0, \sigma^2)$. Variance σ^2 of an individual element of the state vector can be obtained self-consistently, according to $\sigma^2 = g^2\langle\phi^2(w_{\mathrm{FB}}A + \sigma y)\rangle$ with y being a zero mean unit variance Gaussian variable.

The solution X of (5) is represented similarly to the state vector $\bar{x}$ but with the stochastic part X^1 further decomposed into $X_\parallel^1$ and $X_\perp^1$. Defined by $X_\parallel^1 = \alpha(\omega)\bar{x}^1$ and $\langle X_\perp^1 \bar{x}^1\rangle \equiv 0$, these components correspond to the response of internal units to external perturbations in a direction that is parallel, and respectively orthogonal, to the state $\bar{x}^1$. Beyond the technical aspect in the MFT derivation, it is instructive to consider this decomposition in relation to network dynamics. The case of $|X_\parallel^1| \ll |X_\perp^1|$ leads to a time scale difference between output and internal dynamics, which is discussed below Eq. (9). Furthermore, the subspace orthogonal to $\bar{x}^1$, of which $X_\perp^1$ is a member, can be used by adaptive algorithms [26] for improving the stability of training targets that are unstable with the least mean square readout used in this work.

From Eqs. (3) and (5), the correlation between $\bar{x}^1$ and X^1 can be obtained, leading to a linear equation for $\alpha(\omega)$. Realizing that the readout vector w_{out} in the case of $M = 1$ is simply the vector $\bar{r}$, normalized and scaled by the desired output amplitude, we obtain the open loop gain as a mean field estimate of $\langle rr'X\rangle$:

$$G^{\mathrm{OL}}(\omega) = \frac{A\beta_0}{(1 - \beta_1 + i\omega)} \tag{8}$$

with frequency-independent coefficients $\beta_{0,1}$ derived in Ref. [27]. The derivation of (8) required neglecting $X_\perp^1$ due to the following argument: The vectors $\bar{x}^1 = W\bar{r}$ and $X^1 = (1 + i\omega)^{-1}WR'X$ both result from a product with W and are thus jointly Gaussian. Orthogonality to $\bar{x}^1$ thus renders the vector $X_\perp^1$ *independent* of $\bar{x}^1$ and of all its functions.

The single pole of (8) leads to a single (uncanceled) pole $\lambda_{\mathrm{out}} = -(1 - A\beta_0 - \beta_1)$ of the closed loop gain (7) and corresponds to a single eigenvalue of (4). The rest of its spectrum, corresponding to canceled poles, remains intact compared to the open loop system [Figs. 1(a)–1(c)].

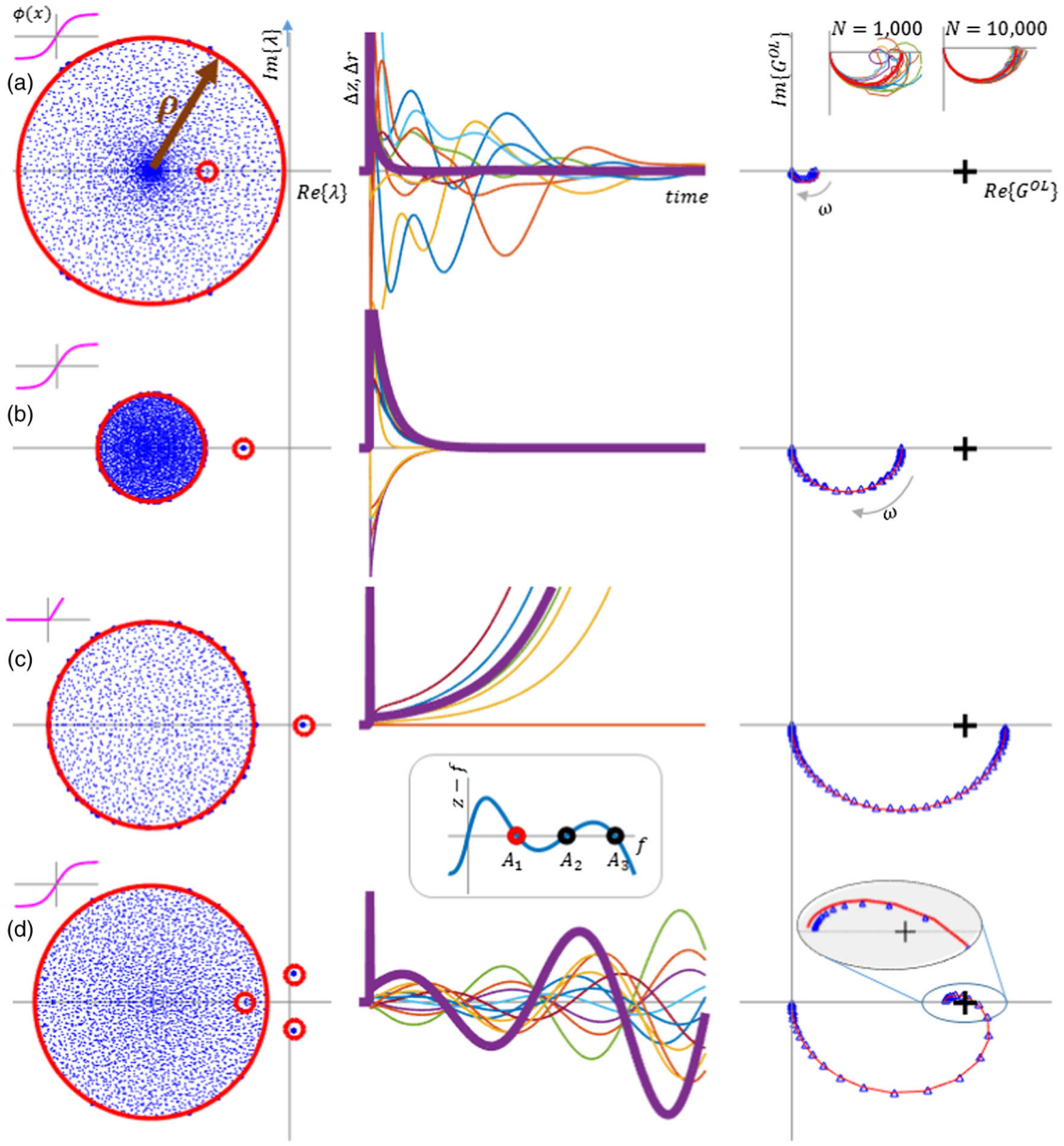

FIG. 1. The analysis of a trained RNN is shown for representative cases compliant with the fading memory property ($\rho < 1$). (a) Internal dynamics are slow compared to network output ($\tau_{\text{net}} > \tau_{\text{out}}$). (b) The opposite case ($\tau_{\text{net}} < \tau_{\text{out}}$), where the internal state is dominated by output feedback. (c) Unstable case ($\tau_{\text{out}} < 0$). (d) Unstable oscillatory solution around one of the targets for $M = 3$. Left: Mean field estimate (red) of the closed loop spectrum compared with a finite size realization (blue dots, $N = 3000$). Middle: A transient response for a δ-like perturbation is shown for both output (thick line) and for ten random neurons (thin lines). Right: A MFT estimation (red) of open loop gain is compared with a finite size realization (blue). The black cross at $1 + 0i$ helps visualize the Nyquist criterion. (a) inset: Finite size effects (for other cases, where ρ is significantly smaller than unity, finite size effects are small and not shown). Parameters: The output value was set to $A = 1$ for all the cases except (d), where $A_{1,2,3} = \{0.5, 1.0, 1.5\}$ (inset) and A_1 is analyzed. Nonlinearity $\phi(x) = \tanh(x)$ was used except (c), for which $\phi(x) = \max(0, x - 0.1)$. The connectivity strength scale g was set to 1.5, 0.5, 1.1, and 1.0 for the cases (a), (b), (c), and (d), respectively.

Interestingly, for a commonly used $\phi(x) = \tanh(x)$ and, more generally, for any sigmoidal activation function $\phi(x)$ with an inflection point at zero, the pole λ_{out} is always negative and the trained system is thus always *stable*. Conversely, it is always *unstable* for a rectified linear activation function $\phi(x) = \max(0, x - x_{\text{th}})$ with positive threshold x_{th}. To check, one expresses λ_{out} as

$$\lambda_{\text{out}} = -\sigma^{-2} g^2 \langle \phi(x')[\phi(x') - x'\phi'(x')] \rangle \tag{9}$$

where $x' = w_{\text{FB}} A + \sigma y$, and observes that the integrand is always non-negative (respectively, nonpositive) for an origin-centered sigmoid (respectively, rectified linear) activation function. The situation with all positive but saturating activation functions (e.g., those investigated in

Ref. [33]) is more complicated, and both stable and unstable settings exist.

The maximum Lyapunov exponent of the system (1) does not necessarily coincide with λ_{out} but rather with $\max(\lambda_{\text{out}}, \rho - 1)$. In particular, for sigmoids mentioned above, $\tau_{\text{out}} \equiv -(\lambda_{\text{out}})^{-1}$ remains finite even for networks at the edge of chaos, where, by definition, the time constant of the internal activity diverges as $\tau_{\text{net}} = (1-\rho)^{-1}$ [3,18]. The case of $\tau_{\text{net}} \gg \tau_{\text{out}}$ is demonstrated in Fig. 1(a) and can explain the experimental observation [22,23] of the robustness of functionally important signals in the presence of highly varying underlying neural activity. From this point of view, the convergence of $G^{\text{OL}}(\omega)$ to its MFT estimate as shown in Fig. 1(a) (inset) can be interpreted as the subspace $X_\perp$ becoming unobservable from the output.

Multiple training targets.—For $M = 1$ the open loop gain (8) has a single pole, which implies that a dc gain smaller than unity $[G^{\text{OL}}(\omega = 0) < 1]$ is a sufficient and necessary condition for the stability of (1). This is not the case for $M > 1$. The least mean square readout weight vector in this case is given by

$$w_{\text{out}} = N^{-1} \sum_{m=1}^{M} k_m \bar{r}_m, \tag{10}$$

where the coefficient vector k is derived from the correlation matrix of the states $\bar{r}$. The open loop gain around the nth fixed point is hence

$$G_n^{\text{OL}}(\omega) = \sum_{m=1}^{M} k_m G_{nm}(\omega) \tag{11}$$

with a diagonal term G_{nn} similar to (8) and cross terms $G_{nm}(\omega) = \langle \bar{r}_m^T R_n' X_n(\omega) \rangle$ which can be brought to a form

$$G_{nm}(\omega) = \frac{K_{nm}(i\omega - z_{nm})}{(i\omega - p_{nn})(i\omega - p_{nm})} \tag{12}$$

with K_{nm}, z_{nm}, p_{nm}, and p_{nn} derived in Ref. [27]. Thus, we conclude that the local dynamics of the output of the closed loop system (7) is governed by an Mth-order ordinary differential equation. This follows from noting that the sum of Eq. (11) renders $G_n^{\text{OL}}(\omega)$ and $G_n^{\text{CL}}(\omega)$ Mth-order rational functions of ω.

The MATLAB code for the mean field calculation of $G^{\text{OL}}(\omega)$ is provided in Ref. [34] along with a detailed derivation of (12) [27].

The higher order of G^{CL} in a multiple fixed point setting implies that the stability condition on the dc gain $G^{\text{OL}}(\omega = 0) < 1$ is no longer sufficient. A counterexample, shown in Fig. 1(d), demonstrates the emergence of complex poles corresponding to unstable oscillatory behavior. Thus, stability requires the evaluation of all M poles of $G^{\text{CL}}(\omega)$. Alternatively, the Nyquist criterion [35,36] can be applied to the open loop system $G^{\text{OL}}(\omega)$ avoiding a direct analysis of $G^{\text{CL}}(\omega)$. Specifically, stability depends on whether the curve $G^{\text{OL}}(\omega)$ from $-\infty$ to $+\infty$ does not encircle the point $1 + 0i$ in the complex plane (black crosses in Fig. 1) [37].

Importantly, stable resonances may also emerge due to the same mechanisms. Resonances are characteristic to a specific steady state $z = A_n$ of the network rather than to the network in general. Figure 2 demonstrates such a state-dependent frequency selectivity in a bistable network. Such selectivity is well known in biological neural circuits [20,21], and our theory suggests that it can emerge as an inherent consequence of having multiple steady states (e.g., fixed points) rather than due to some dedicated frequency adaptation process. Remarkably, resonance emerges by perturbing through an arbitrary input w_{in} in (1), and not only through w_{FB}, since the resonant eigenvalues shown in Fig. 2 also dictate the slowest time scale of the system as a whole, regardless of the input details.

While no fully analytical treatment for the resonance characteristics is available, we note that we commonly observed resonance frequencies in the range of $\omega_0 \approx 0.1$–0.5. Interestingly, Rajan, Abbott, and Sompolinsky [4] predicted enhanced chaos suppression by stimuli in a very similar frequency range, indicating a possible connection between the two phenomena. Supplemental Material (Sec. 2) contains several bounds on these frequencies, but a full analysis is beyond the scope of the current work.

Naturally, many questions arise concerning a generalization of these results to more complex settings, such as input-dependent outputs, time-varying targets, advanced adaptive training algorithms, and dynamics in the noisy (chaotic) regime beyond the fading memory domain [1,26,38]. The initial investigation of a simple dynamical task [15,39] shows that the local stability around fixed points determines training success and failure [27], indicating the relevance of our work to more complex, time-dependent settings. The derivation of an analytical solution

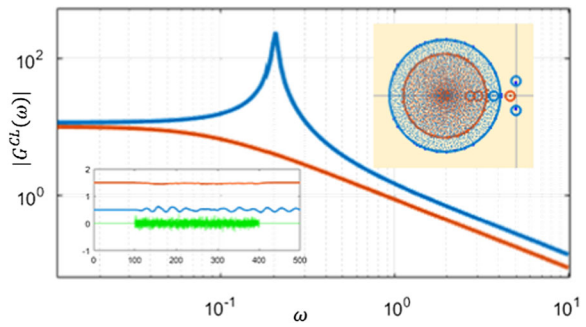

FIG. 2. Network with stable fixed points at $A_1 = 0.5$ (blue) and $A_3 = 1.5$ (orange) exhibits frequency selectivity around the lower fixed point A_1, while at the higher fixed point A_3 no such selectivity exists. G^{CL} for both cases is shown along with the spectrum (top inset) and transient response for the same white noise input (green) delivered through w_{in} to both fixed points. The settings of Fig. 1(d) were used, except that here $g = 0.9$.

for such a case (left for a future work) requires an extension of the dynamical mean field theory [3,4] to a nonstationary case. Obviously, there also exist failure mechanisms that are not determined by local dynamics; in particular, there is an inherent trade-off between stability and sensitivity to external input. As for chaotic networks, our analysis indicates a smooth transition between chaotic and fading memory regime. In particular, according to Eq. (9), the output feedback loop remains *formally* stable at the edge of chaos, while the assumption of $\rho < 1$ which was used to derive this equation becomes invalid. Numerical simulations of this setting show that the output becomes noisy but remains stable [27].

In conclusion, we considered high-dimensional networks adapted to produce a desired low-dimensional output. The output is being interpreted here as a firing rate but can also stand for stable gene expression [40] or a variety of other observables [41]. In all these cases, the network's internal state remains high dimensional and hard to interpret or investigate directly. The method of combining a mean field approach with system analysis presented here enables predictions ranging from instability to extreme robustness of the network of interest.

We thank Larry Abbott, Naama Brenner, Lukas Geyrhofer, Vishwa Goudar, Leonid Mirkin, Daniel Soudry, and Merav Stern for their valuable comments. O. B. is supported by a Marie Curie Career Integration Grants, Seventh Framework Program (FP7) of the European Commission (Grant No. 2013-618543), by Fondation Adelis, and by the Israel Science Foundation (Grant No. 346/16).

*arivkind@tx.technion.ac.il
†omri.barak@gmail.com

[1] V. Mante, D. Sussillo, K. V. Shenoy, and W. T. Newsome, Nature (London) **503**, 78 (2013).
[2] Y. LeCun, Y. Bengio, and G. Hinton, Nature (London) **521**, 436 (2015).
[3] H. Sompolinsky, A. Crisanti, and H. J. Sommers, Phys. Rev. Lett. **61**, 259 (1988).
[4] K. Rajan, L. F. Abbott, and H. Sompolinsky, Phys. Rev. E **82**, 011903 (2010).
[5] M. Stern, H. Sompolinsky, and L. F. Abbott, Phys. Rev. E **90**, 062710 (2014).
[6] J. Kadmon and H. Sompolinsky, Phys. Rev. X **5**, 041030 (2015).
[7] M. Massar and S. Massar, Phys. Rev. E **87**, 042809 (2013).
[8] J. J. Hopfield, Proc. Natl. Acad. Sci. U.S.A. **79**, 2554 (1982).
[9] E. Gardner, J. Phys. A **21**, 257 (1988).
[10] R. Ben-Yishai, R. L. Bar-Or, and H. Sompolinsky, Proc. Natl. Acad. Sci. U.S.A. **92**, 3844 (1995).
[11] O. V. Popovych, C. Hauptmann, and P. A. Tass, Phys. Rev. Lett. **94**, 164102 (2005).
[12] K. Pyragas, Phys. Lett. A **170**, 421 (1992).
[13] E. Ott, C. Grebogi, and J. A. Yorke, Phys. Rev. Lett. **64**, 1196 (1990).
[14] F. Carnevale, V. de Lafuente, R. Romo, O. Barak, and N. Parga, Neuron **86**, 1067 (2015).
[15] D. Sussillo and O. Barak, Neural Comput. **25**, 626 (2013).
[16] L. Abbott, B. DePasquale, and R.-M. Memmesheimer, Nat. Neurosci. **19**, 350 (2016).
[17] S. A. Neymotin, G. L. Chadderdon, C. C. Kerr, J. T. Francis, and W. W. Lytton, Neural Comput. **25**, 3263 (2013).
[18] Y. Ahmadian, F. Fumarola, and K. D. Miller, Phys. Rev. E **91**, 012820 (2015).
[19] D. V. Buonomano, Neuron **63**, 423 (2009).
[20] G. Buzsaki, *Rhythms of the Brain* (Oxford University, New York, 2006).
[21] S. L. Brincat and E. K. Miller, Nat. Neurosci. **18**, 576 (2015).
[22] U. Rokni, A. G. Richardson, E. Bizzi, and H. S. Seung, Neuron **54**, 653 (2007).
[23] S. Druckmann and D. B. Chklovskii, Curr. Biol. **22**, 2095 (2012).
[24] W. Maass, T. Natschläger, and H. Markram, Neural Comput. **14**, 2531 (2002).
[25] H. Jaeger, German National Research Center for Information Technology, GMD Technical Report No. 148 (2001).
[26] D. Sussillo and L. F. Abbott, Neuron **63**, 544 (2009).
[27] See Supplemental Material at http://link.aps.org/supplemental/10.1103/PhysRevLett.118.258101, which includes Refs. [28–31], for (i) fading memory property and rank one perturbations, (ii) derivation of open loop gain, and (iii) discussion about extending this work beyond fixed points.
[28] K. J. Aström and R. M. Murray, in Ref. [27], Chap. 7.
[29] G. Hennequin, T. P. Vogels, and W. Gerstner, Neuron **82**, 1394 (2014).
[30] I. B. Yildiz, H. Jaeger, and S. J. Kiebel, Neural Netw. **35**, 1 (2012).
[31] G. Manjunath and H. Jaeger, Neural Comput. **25**, 671 (2013).
[32] K. J. Aström and R. M. Murray, *Feedback Systems: An Introduction for Scientists and Engineers* (Princeton University, Princeton, NJ, 2010), Chap. 6.
[33] F. Mastrogiuseppe and S. Ostojic, PLoS Comput. Biol. **13**, e1005498 (2017).
[34] See Supplemental Material at http://link.aps.org/supplemental/10.1103/PhysRevLett.118.258101 for the MATLAB code.
[35] H. Nyquist, Bell Syst. Tech. J. **11**, 126 (1932).
[36] K. J. Aström and R. M. Murray, in Ref. [27], Chap. 9.
[37] Because of the echo state property, the open loop system is stable, and the criterion is necessary and sufficient.
[38] T. Matsuki and K. Shibata, *Reward-Based Learning of a Memory-Required Task Based on the Internal Dynamics of a Chaotic Neural Network* (Springer, New York, 2016), pp. 376–383.
[39] G. M. Hoerzer, R. Legenstein, and W. Maass, Cereb. Cortex **24**, 677 (2014).
[40] S. Ciliberti, O. C. Martin, and A. Wagner, Proc. Natl. Acad. Sci. U.S.A. **104**, 13591 (2007).
[41] B. Barzel and A.-L. Barabási, Nat. Phys. **9**, 673 (2013).